Supplement of Atmos. Chem. Phys., 26, 15583–15592, 2026
https://doi.org/10.5194/acp-26-15583-2026-supplement
© Author(s) 2026. CC BY 4.0 License.



Atmospheric Chemistry and Physics
Open Access
EGU

*Supplement of*

# Uncovering the seasonal trends of VOC production from ozonolysis of seawater

**Frances E. Hopkins et al.**

*Correspondence to:* Frances E. Hopkins (fhop@pml.ac.uk)

The copyright of individual parts of the supplement might differ from the article licence.

# Supporting Information

## Methods

### Seawater sampling

Surface seawater was routinely collected from the Western Channel Observatory station L4 using the rosette on the RV *Plymouth Quest* at a mean depth of **1.8 ± 0.3 m** (range: **1.4 m**) between **08:00–10:00** local time. Seawater was transferred directly from Niskin bottles into acid-washed, thoroughly rinsed glass bottles using Tygon tubing and gas-sensitive techniques. Bottles were allowed to overflow **3×** before sealing with a ground-glass stopper, minimizing bubbles and gas loss. Samples were transported to the laboratory in a dark, insulated cool box and analysed as soon as possible to limit DOM alteration (**59%** within **3 h**, **94%** within **24 h**).

Sampling campaigns covered contrasting seasons:

- **Late winter/spring:** 14 Feb 2017 – 03 May 2017
- **Autumn/winter:** 04 Sep 2018 – 05 Nov 2018
- **Summer/autumn:** 15 Jun 2020 – 12 Oct 2020

### Bubble-column reactor

Experiments used a custom 1.45 L cylindrical borosilicate glass column fitted with a fine glass-frit sparger (acid-washed and rinsed with ultrapure water between samples) (Figure S1). A ~200 mL volume below the sparger housed a gas inlet and stopcock. With the stopcock closed, **1.2 L** of sample was siphoned above the sparger using silicone tubing to minimize bubble formation, leaving a **205 mL** headspace containing the gas outlet.

Compressed artificial air (BOC BTCA 178) served as the carrier gas and was scrubbed for organics via a custom Pt catalyst at **450 °C**. A flow of **150 n mL min$^{-1}$** (1 atm, 0 °C; ≈ **165 mL min$^{-1}$** at room temperature) was set with mass-flow controllers (Bronkhorst EL-FLOW Select series). Opening the stopcock directed the gas through the frit, producing a dense turbulent plume of bubbles (~**0.5 mm** diameter each; ~**3 mL** total bubble volume) rising through the sample. Bubble residence time in water was ~**1.2 s**.

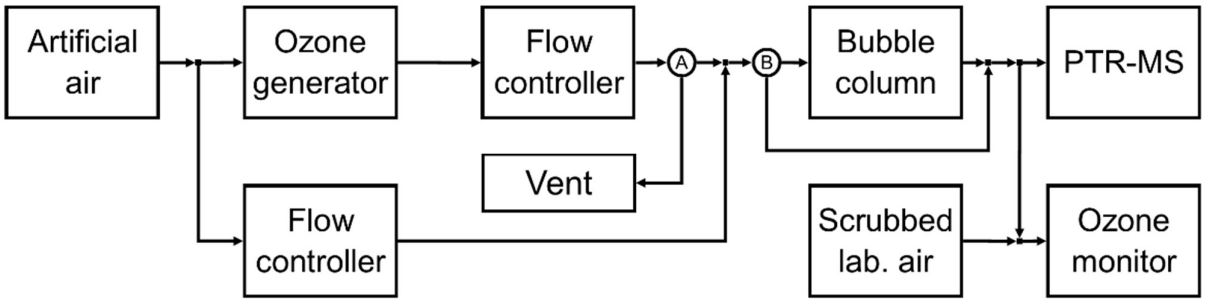



**Figure S1. Schematic of the turbulent ozonolysis experimental setup. Arrows indicate flow; A and B denote three-way valves.**

## Ozone generation and measurement

$O_3$ was generated from the artificial air using a corona-discharge source (Enaly 1000BT-12) and mixed into the carrier stream to achieve **1–15 ppmv** (rarely >3 ppmv). Although these $O_3$ levels exceed typical marine boundary layer (MBL) values (×25–150), the response was experimentally linear below ~**4 ppmv (Figure S2)**. Headspace $O_3$ was measured with a dual-channel (simultaneous blank correction) monitor (2B Technologies Model 205), providing high temporal resolution. The monitor's inlet draws ~**2 L min$^{-1}$**; to supply the balance, a tee provided additional $O_3$-scrubbed dilution air vented to the lab, yielding an effective dilution of ~**93–98%** and necessitating elevated inlet $O_3$ concentrations. Total flows (monitor + dilution air) were verified with a digital bubble meter (Gilian Gilibrator-2). The $O_3$ generator and monitor were warmed for **1–2 h** with artificial air to stabilize. PFA tubing (3.2 mm ID) connected the $O_3$ generator to the column and the column to the monitor; three-way valves and MFCs were stainless steel.

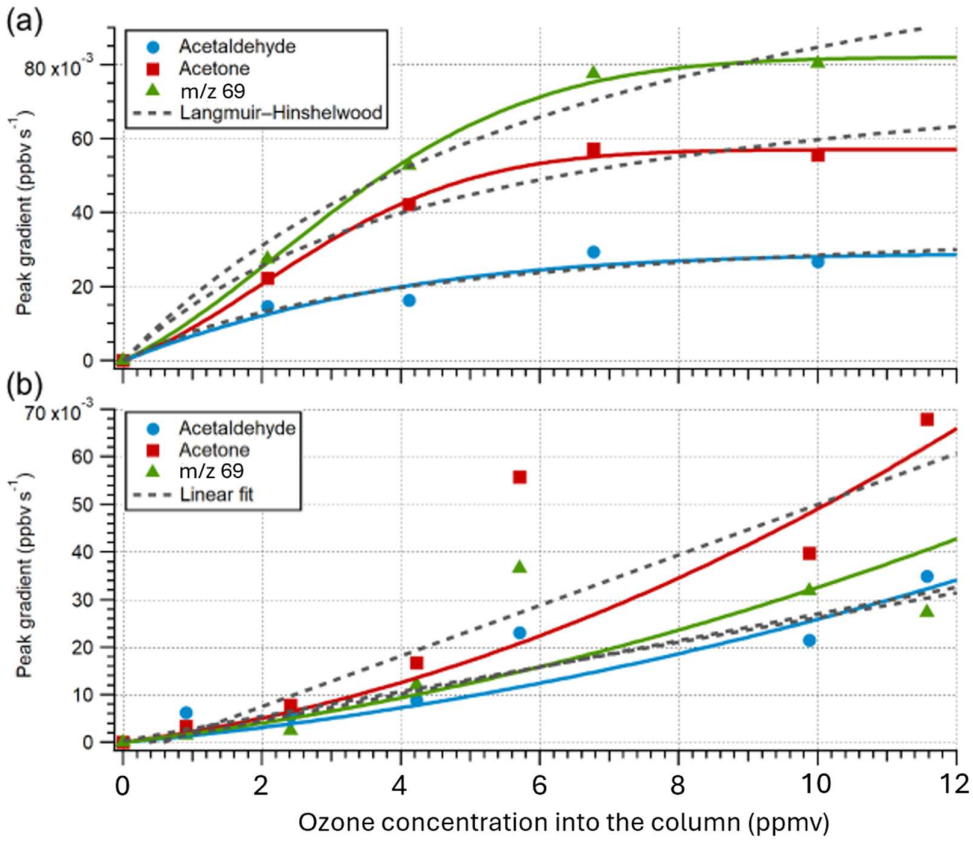



Figure S2. The effect of increasing ozone concentration with surface seawater collected from station L4 (Western Channel Observatory) using ozone heterogeneous oxidation on (a) the rate of VOC production from April 2017, and (b) the rate of VOC production from October 2020. In (b) the 5.7 ppmv measurement was omitted in regression analysis for all VOCs.

The impact of iodide ($I^-$) on VOC production was tested by adding increasing concentrations of $I^-$ to natural seawater (Figure S3). A slight reduction in acetaldehyde and acetone peak height and production ratios (Figure S3) with increasing $I^-$ concentration demonstrates the competition between $I^-$ and VOC-producing DOM for available ozone. The production of m/z 69 was unchanged, which could imply that m/z 69 production occurs at the interface, while acetone and acetaldehyde production occurs in bulk water where there is more competition with iodide.

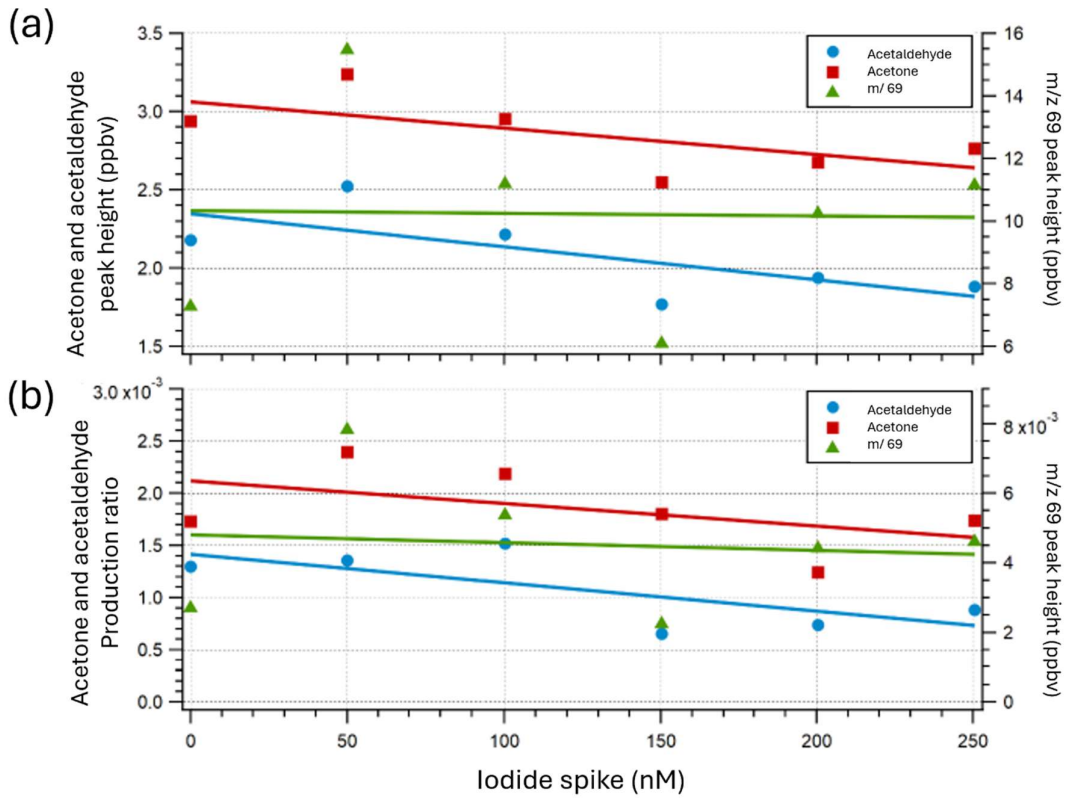



Figure S3. Influence of additional iodide on VOC production from natural seawater (a) VOC peak heights and (b) VOC production ratios.

## PTR-MS measurements

Headspace VOCs were quantified with a PTR-MS. All line connections between column headspace and instrument were 3.2 mm ID PFA. Core monitored masses included methanol (*m/z* 33), acetaldehyde (*m/z* 45), acetone (*m/z* 59), DMS (*m/z* 63), and isoprene (*m/z* 69). Additional masses varied by campaign (Table S1); details of masses, fragment ion ratios from literature, and dwell times are provided in Table S2. For isoprene, *m/z* 39 and 41 (fragments) were included (Schwarz et al., 2009). Overall temporal resolution was 3.1–7.7 s (0.13–0.27 Hz). Internally corrected PTR-MS mixing ratios (ppbv) were used. Method parameters are in Table S3.

**Table S1. PTR-MS measurement frequencies, temporal resolutions and mass list by campaign.**

| Campaign | Frequency (Hz) | Time (s) | Notes |
|---|---|---|---|
| 2017 | 0.13 | 7.7 | Added *m/z* 21, 32, 33, 39, 42, 42, 43, 45, 47, 59, 60, 61, 63, 69, 71, 79, 93, 107, 137 |
| 2018 beginning | 0.32 | 3.1 | Removed *m/z* 39, 42, 43, 47, 60, 61, 71, 79, 93, 107, 137<br>Added *m/z* 37 |
| 2018 end | 0.27 | 3.7 | Added *m/z* 39 with increased dwell time<br>Increased *m/z* 32 and 37 dwell times |
| 2020 beginning | 0.16 | 6.2 | Added *m/z* 43, 47, 57, 61, 73 |
| 2020 end | 0.14 | 7.2 | Added *m/z* 55, 87 |

**Table S2. Target masses, expected compounds, literature ion ratios, formulas, and dwell times [1,2].**

| Mass-charge ratio | Expected compound/s | Literature ion ratio (%) | Structural formula | Residence time (ms) |
|---|---|---|---|---|
| 21 | Hydronium | - | $H_3{}^{18}O^+$ | 50 |
| 32 | Oxygen | - | $O_2{}^+$ | 20–50 |
| 33 | Methanol | 100[b] | $CH_3OH_2{}^+$ | 500 |
| 37 | Water dimer | - | $H_2O.H_3O^+$ | 20–50 |
| 39 | Isoprene (fragment)<br>Isotopic water dimer<br>Pentanal (fragment) | 10[b]<br>-<br>2[b] | $CH_2CCH^+$<br>$H_2{}^{18}O.H_3O^+$ / $H_2O.H_3{}^{18}O^+$ | 50–500 |
| 41 | Isoprene (fragment)<br>Propanal (fragment)<br>Pentanal (fragment) | 39[b]<br>4[b]<br>23[b] | $CH_2CCH_3{}^+$ | 500 |
| 43 | Propene<br>Acetone (fragment) | -<br>10[a] | | 500 |
| 45 | Acetaldehyde<br>Pentanal | 100[b]<br>2[b] | $CH_3COOH_2{}^+$ | 500 |
| 47 | Formic acid | - | | 500 |
| 55 | Butanal (fragment)<br>Butadiene | 57[a], 90[b]<br>- | | |
| 57 | Butene | 100[a] | | 500 |
| 59 | Acetone<br>Propanal | 90[a], 98[b]<br>100[a], 89[b] | $CH_3COCH_3{}^+$<br>$CH_3CH_2CH_2O^+$ | 500 |
| 61 | Acetic acid | - | | 500 |
| 63 | DMS | 100[a] | $CH_3SHCH_3{}^+$ | 500 |
| 69 | Isoprene<br>Pentanal (fragment) | 100[a],46[b]<br>78[a], 68[b] | $CH_2C(CH_3)CHCH_3{}^+$ | 500 |
| 73 | Butanal<br>Butanone | 43[a], 7[b]<br>- | C4H8O | 500 |
| 87 | Pentanal<br>Pentanone | 87[a], 5[b],<br>100[a] | | 500 |

**Table S3. PTR-MS method parameters.**

| Parameter | Value |
|---|---|
| Drift chamber pressure (mBar) | 2.21 |
| Drift chamber voltage (true) (V) | 690 |
| Drift chamber temperature (°C) | 80 |
| $H_2O$ mass flow controller (mL $min^{-1}$) | 5 |
| Inlet flow rate (mL $min^{-1}$) | 80–120 |
| Inlet temperature (°C) | 80 |

## Experimental Sequence

Each experiment cycled through four stages, with $O_3$ and VOCs measured continuously:

1. **Stage 1 — $O_3$ input:** Bypass column to measure generator output ($O_3$ input).
2. **Stage 2 — Dry VOC blank:** Bypass column for a gas-phase VOC blank.
3. **Stage 3 — Air purge:** Pass artificial air through the water sample. This strips dissolved VOCs to the headspace and flushes the headspace to an approximate steady state with the underlying water. Of the monitored VOCs, only isoprene typically declines appreciably during this stage due to its low solubility and efficient purging.
4. **Stage 4 — Oxidation:** Add $O_3$ to the carrier stream to initiate ozonolysis.

Typically, two Milli-Q water runs were performed prior to triplicate seawater samples to verify column cleanliness and provide a humid VOC blank.

## Reactant-addition experiments

To probe precursor classes and product signatures, select reactants were added to **aged seawater** (stored ~**1 month**, dark, gas-tight glass, **20 °C**) in the bubble column. Aged seawater was preferred over Milli-Q to preserve salinity, which influences bubble size distributions and thus gas–liquid interfacial area and reaction rates (FwarnF, 1975).

- **Phytoplankton:** *Emiliania huxleyi* Rutgers 607 was grown on-site to senescence (mature, not lysing) and added directly by briefly removing the column cap (~**10 s**) and pipetting **5–20 mL** culture onto the water surface. Dilutions targeted final cell abundances within ambient seawater ranges ($10^2$ – $10^4$ cells $mL^{-1}$) (assuming no algal cells in the aged seawater).
- **NOM:** Suwannee River natural organic matter (International Humic Substances Society) was dissolved in **10 mL** aged seawater and poured into the column to yield **0–10 mg $L^{-1}$**.

- **Fatty acids:** Oleic and nonanoic acids (**0–400 µL**) were injected directly onto the water surface via the column side arm.

- **Iodide:** KI (Acros Organics, >99%) was dissolved in Milli-Q to prepare a **0.6 mM** $I^-$ standard (serial dilution). Aliquots (**0–500 µL**) were injected into the seawater; aged seawater was avoided as solvent to minimize background $I^-$. Natural surface seawater $I^-$ is ~**100 nM** [3]; each **100 µL** addition here increased [$I^-$] by **50.1 nM**.

### Calibration and limits of detection (LOD)

VOC data were averaged to 1 min intervals and converted using calibration factors derived from gas-phase calibrations with a certified standard (Apel-Riemer Environmental, 500 ppbv for all VOCs here). $O_3$ data were also 1-min averaged, corrected for zero drift, and adjusted for the scrubbed dilution air. The $O_3$ monitor was calibrated during routine servicing, cross-checked against other instruments, or verified with a portable $O_3$ source (2B Technologies Model 306). Under standard operation, calibration drift was negligible.

The limits of detection (LOD) were defined as 3σ following Wohl et al (2019). Using seawater-equivalent LODs reported for the PTR-MS system (0.51 nmol $L^{-1}$ for acetaldehyde, 1.32nmol $L^{-1}$ for acetone and 1.74 pmol $L^{-1}$ for m/z 69), the corresponding equilibrium gas-phase concentrations are estimated to be 0.03, 0.04 and 0.08 ppbv, respectively. These values are substantially lower than the VOC enhancements observed during the ozonolysis experiments.

**Table S4. Instrument calibration factors.**

| Instrument | Compound | Calibration factor |
|---|---|---|
| PTR–MS | Methanol | 0.447±0.053 |
| | Acetaldehyde | 0.820±0.042 |
| | Acetone | 0.949±0.103 |
| | DMS | 0.549±0.146 |
| | Isoprene | 0.138±0.012 |
| $O_3$ monitor | $O_3$ | n/a, frequently updated with internal correction |

## Data processing

### Peak data

Figure S2 shows a representative time series (1-min resolution) for acetaldehyde, acetone, isoprene, and $O_3$ during ozonolysis of one sample; similar plots were used to extract peak metrics.

We define two primary metrics from **Stage 4**:

- **VOC peak height (ppbv):** The difference between the steady-state headspace concentration at the end of Stage 3 and the maximum concentration during Stage 4.
- **Initial gradient (ppbv $s^{-1}$):** The maximum initial rate of increase prior to the peak maximum, obtained by linear regression over the earliest, linear segment.

The area under the peak corresponds to the total VOC produced from the available DOM; however, full consumption typically required **>1.5 h**, so peak area was seldom integrated to maintain $O_3$-input stability. Instead, VOC production was quantified using the maximum PTR-MS signal increase (peak height) following ozone addition to the bubble column as this provided a robust measure of VOC production that is less sensitive to variations in system flushing and response time that integration of the peak. The small apparent step in peak height between ~14:50–14:51 in Figure S4, relative to the initial slope (green line), is an artefact of 1-min averaging rather than reaction kinetics (see Sect. 2.5.3).

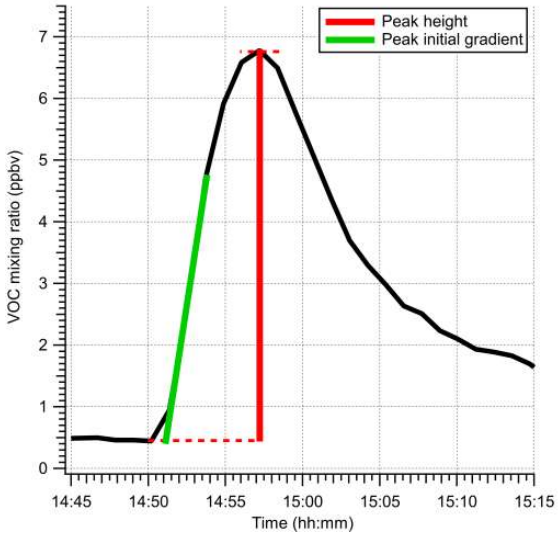



**Figure S4.** Example determination of VOC peak height and initial gradient.

## Headspace mass balance and production rate

The headspace concentration of a VOC is governed by production at the air–water interface and advective removal by the purge flow. The differential equation is:

$$\frac{dC_{\mathrm{VOC}}}{dt} = \frac{P_{\mathrm{VOC}}\, A_{\mathrm{bub}}}{V_{\mathrm{air}}} - \frac{F_{\mathrm{air}}}{V_{\mathrm{air}}}\, C_{\mathrm{VOC}} \qquad \text{(S1)}$$

where $C_{VOC}$ is the headspace concentration (ppbv), $P_{VOC}$ is the areal production flux (mol m$^{-2}$ s$^{-1}$), $A_{bub}$ is interfacial area (m$^2$), $V_{air}$ is headspace volume (m$^3$), and $F_{air}$ is the gas flow (m$^3$ s$^{-1}$).

At the earliest times of Stage 4, $C_{VOC}$ is still small, so the purge-loss term is minor. Thus,

$$P_{VOC} \approx \frac{V_{air}}{A_{bub}} \left(\frac{dC_{VOC}}{dt}\right)_{initial} \quad \text{(S2)}$$

### $O_3$ deposition flux

$O_3$ is supplied at a constant inlet concentration, and the deposition flux into the sample is:

$$D_{F,O_3} = \frac{F_{air}\left(C_{O_3,G} - C_{O_3,H}\right)}{A_{bub}} \approx \frac{F_{air}\, C_{O_3,G}}{A_{bub}} \text{(early times; } O_3 \text{ limiting)} \quad \text{(S3)}$$

where $C_{O_3,G}$ and $C_{O_3,H}$ are inlet and headspace $O_3$, respectively. Early in Stage 4, headspace $O_3 \approx 0$ when DOM or reduced sulfur species rapidly consume $O_3$, justifying the approximation. Wall losses on stainless steel, glass, and PFA are assumed negligible relative to sample uptake.

### VOC–$O_3$ production ratio

Dividing Eq. S2 by Eq. S3 yields a dimensionless "production ratio" of VOC produced per $O_3$ taken up:

$$\frac{P_{VOC}}{D_{F,O_3}} \approx \frac{V_{air}}{F_{air}} \frac{(dC_{VOC}/dt)_{initial}}{C_{O_3,G}} \quad \text{(S4)}$$

*Note:* $A_{bub}$ cancels, so uncertainty in interfacial area does not affect this ratio.

## References


1 Warneke, C., De Gouw, J. A., Kuster, W. C., Goldan, P. D. & Fall, R. Validation of atmospheric VOC measurements by proton-transfer-reaction mass spectrometry using a gas-chromatographic preseparation method. *Environmental science & technology* **37**, 2494-2501 (2003).

2 Schwarz, K., Filipiak, W. & Amann, A. Determining concentration patterns of volatile compounds in exhaled breath by PTR-MS. *Journal of Breath Research* **3**, 027002 (2009).

3 Chance, R., Baker, A. R., Carpenter, L. & Jickells, T. D. The distribution of iodide at the sea surface. *Environmental Science: Processes & Impacts* **16**, 1841-1859 (2014).

# Data

**Table S5. VOC data (ppbv) presented in Figure 1**

| Timestamp_ave | me45_ave | me59_ave | me69_ave |
|---|---|---|---|
| 05/11/2018 14:25 | 2.144 | 1.116 | 0.104 |
| 05/11/2018 14:26 | 1.873 | 0.911 | 0.093 |
| 05/11/2018 14:28 | 1.265 | 0.619 | 0.079 |
| 05/11/2018 14:29 | 1.088 | 0.529 | 0.077 |
| 05/11/2018 14:30 | 0.984 | 0.474 | 0.069 |
| 05/11/2018 14:31 | 0.901 | 0.444 | 0.075 |
| 05/11/2018 14:32 | 9.535 | 5.858 | 0.453 |
| 05/11/2018 14:33 | 9.670 | 2.604 | 0.603 |
| 05/11/2018 14:35 | 9.637 | 2.220 | 0.588 |
| 05/11/2018 14:36 | 9.934 | 2.258 | 0.583 |
| 05/11/2018 14:37 | 10.014 | 2.554 | 0.583 |
| 05/11/2018 14:38 | 9.756 | 2.869 | 0.592 |
| 05/11/2018 14:39 | 9.380 | 3.086 | 0.576 |
| 05/11/2018 14:40 | 8.763 | 3.281 | 0.544 |
| 05/11/2018 14:42 | 7.813 | 3.416 | 0.527 |
| 05/11/2018 14:43 | 7.098 | 3.557 | 0.551 |
| 05/11/2018 14:44 | 6.513 | 3.475 | 0.487 |
| 05/11/2018 14:45 | 6.271 | 3.584 | 0.492 |
| 05/11/2018 14:46 | 6.028 | 3.482 | 0.499 |
| 05/11/2018 14:47 | 5.796 | 3.485 | 0.461 |
| 05/11/2018 14:49 | 5.781 | 3.561 | 0.460 |
| 05/11/2018 14:50 | 5.581 | 3.494 | 0.443 |
| 05/11/2018 14:51 | 5.680 | 3.885 | 0.945 |
| 05/11/2018 14:52 | 6.223 | 5.014 | 2.660 |
| 05/11/2018 14:53 | 6.666 | 5.500 | 4.699 |
| 05/11/2018 14:54 | 7.087 | 5.289 | 5.914 |
| 05/11/2018 14:56 | 7.280 | 4.889 | 6.585 |
| 05/11/2018 14:57 | 7.322 | 4.635 | 6.781 |
| 05/11/2018 14:58 | 7.301 | 4.449 | 6.497 |
| 05/11/2018 14:59 | 7.328 | 4.247 | 5.776 |
| 05/11/2018 15:00 | 7.290 | 4.276 | 5.067 |
| 05/11/2018 15:01 | 6.997 | 4.118 | 4.358 |
| 05/11/2018 15:03 | 6.777 | 4.020 | 3.697 |
| 05/11/2018 15:04 | 6.677 | 3.959 | 3.299 |
| 05/11/2018 15:05 | 6.624 | 3.883 | 2.980 |
| 05/11/2018 15:06 | 6.453 | 3.722 | 2.635 |
| 05/11/2018 15:07 | 6.332 | 3.701 | 2.510 |
| 05/11/2018 15:08 | 6.339 | 3.669 | 2.236 |
| 05/11/2018 15:10 | 6.193 | 3.601 | 2.100 |
| 05/11/2018 15:11 | 6.235 | 3.618 | 1.934 |
| 05/11/2018 15:12 | 6.145 | 3.623 | 1.888 |
| 05/11/2018 15:13 | 6.115 | 3.567 | 1.829 |

| | | | |
|---|---|---|---|
| 05/11/2018 15:14 | 5.753 | 3.354 | 1.694 |
| 05/11/2018 15:15 | 5.536 | 3.189 | 1.473 |
| 05/11/2018 15:17 | 5.088 | 2.957 | 1.335 |
| 05/11/2018 15:18 | 4.882 | 2.810 | 1.256 |
| 05/11/2018 15:19 | 4.716 | 2.674 | 1.120 |
| 05/11/2018 15:20 | 4.560 | 2.667 | 1.115 |
| 05/11/2018 15:21 | 4.632 | 2.741 | 1.043 |
| 05/11/2018 15:22 | 4.579 | 2.658 | 1.015 |
| 05/11/2018 15:24 | 4.528 | 2.614 | 0.978 |
| 05/11/2018 15:25 | 4.465 | 2.649 | 0.978 |
| 05/11/2018 15:26 | 4.492 | 2.553 | 0.921 |
| 05/11/2018 15:27 | 4.392 | 2.576 | 0.914 |
| 05/11/2018 15:28 | 4.356 | 2.577 | 0.889 |
| 05/11/2018 15:29 | 4.252 | 2.497 | 0.855 |
| 05/11/2018 15:31 | 3.857 | 3.250 | 0.441 |
| 05/11/2018 15:32 | 2.508 | 1.888 | 0.132 |
| 05/11/2018 15:33 | 2.616 | 1.664 | 0.115 |
| 05/11/2018 15:34 | 2.256 | 1.276 | 0.095 |
| 05/11/2018 15:35 | 2.085 | 1.120 | 0.098 |
| 05/11/2018 15:36 | 1.917 | 0.968 | 0.085 |
| 05/11/2018 15:38 | 1.849 | 0.903 | 0.090 |
| 05/11/2018 15:39 | 1.543 | 0.798 | 0.084 |
| 05/11/2018 15:40 | 1.036 | 0.557 | 0.077 |

**Table S6. Ozone data (ppbv) presented in Figure 1**

| Time_1min | O3_ppb_1min |
|---|---|
| 05/11/2018 14:25 | 2118.41 |
| 05/11/2018 14:26 | 2121.49 |
| 05/11/2018 14:27 | 1594.86 |
| 05/11/2018 14:28 | 32.7017 |
| 05/11/2018 14:29 | 35.7829 |
| 05/11/2018 14:30 | 8.05217 |
| 05/11/2018 14:31 | -8.6376 |
| 05/11/2018 14:32 | 21.404 |
| 05/11/2018 14:33 | 7.28188 |
| 05/11/2018 14:34 | -14.0297 |
| 05/11/2018 14:35 | 16.7822 |
| 05/11/2018 14:36 | -0.934627 |
| 05/11/2018 14:37 | -21.2191 |
| 05/11/2018 14:38 | 46.0535 |
| 05/11/2018 14:39 | -3.75905 |
| 05/11/2018 14:40 | -13.7729 |
| 05/11/2018 14:41 | -28.6653 |
| 05/11/2018 14:42 | -32.2601 |
| 05/11/2018 14:43 | 16.7822 |
| 05/11/2018 14:44 | -18.1379 |

| | |
|---|---|
| 05/11/2018 14:45 | 8.30894 |
| 05/11/2018 14:46 | 2.40333 |
| 05/11/2018 14:47 | -10.1782 |
| 05/11/2018 14:48 | -15.827 |
| 05/11/2018 14:49 | -2.98875 |
| 05/11/2018 14:50 | 37.0667 |
| 05/11/2018 14:51 | 28.0799 |
| 05/11/2018 14:52 | 2.91686 |
| 05/11/2018 14:53 | 26.0258 |
| 05/11/2018 14:54 | 2.40333 |
| 05/11/2018 14:55 | 17.2957 |
| 05/11/2018 14:56 | 66.5948 |
| 05/11/2018 14:57 | 63.2568 |
| 05/11/2018 14:58 | 70.4463 |
| 05/11/2018 14:59 | 114.353 |
| 05/11/2018 15:00 | 106.907 |
| 05/11/2018 15:01 | 128.475 |
| 05/11/2018 15:02 | 177.261 |
| 05/11/2018 15:03 | 220.654 |
| 05/11/2018 15:04 | 226.56 |
| 05/11/2018 15:05 | 212.181 |
| 05/11/2018 15:06 | 237.858 |
| 05/11/2018 15:07 | 287.157 |
| 05/11/2018 15:08 | 296.657 |
| 05/11/2018 15:09 | 282.535 |
| 05/11/2018 15:10 | 287.157 |
| 05/11/2018 15:11 | 313.603 |
| 05/11/2018 15:12 | 359.051 |
| 05/11/2018 15:13 | 341.591 |
| 05/11/2018 15:14 | 366.497 |
| 05/11/2018 15:15 | 249.155 |
| 05/11/2018 15:16 | 141.57 |
| 05/11/2018 15:17 | 40.9182 |
| 05/11/2018 15:18 | 61.4595 |
| 05/11/2018 15:19 | 11.3901 |
| 05/11/2018 15:20 | -5.55641 |
| 05/11/2018 15:21 | -18.3947 |
| 05/11/2018 15:22 | -10.6917 |
| 05/11/2018 15:23 | -14.8 |
| 05/11/2018 15:24 | 23.2014 |
| 05/11/2018 15:25 | -42.7874 |
| 05/11/2018 15:26 | -18.9082 |
| 05/11/2018 15:27 | -16.3406 |
| 05/11/2018 15:28 | -31.7465 |
| 05/11/2018 15:29 | 0.605967 |
| 05/11/2018 15:30 | -5.81318 |
| 05/11/2018 15:31 | -15.0567 |
| 05/11/2018 15:32 | 137.462 |

| | |
|---|---|
| 05/11/2018 15:33 | 1958.96 |
| 05/11/2018 15:34 | 2029.31 |
| 05/11/2018 15:35 | 2040.35 |
| 05/11/2018 15:36 | 2063.98 |
| 05/11/2018 15:37 | 2136.13 |
| 05/11/2018 15:38 | 2118.92 |
| 05/11/2018 15:39 | 2027.26 |

175

**Table S7. PTR-MS data presented in Figure 2a and 2b (m/z 45, 49, 69 = peak height, m/zXX_grad = peak gradient, m/zXX_gradSD = standard devaition)**

| DoY | m/z45 | m/z45_SD | m/z59_ | m/z59_SD | m/z69 | m/z69_SD | m/z45_grad | m/z45_gradSD | m/z59_grad | m/z59_gradSD | m/z69_grad | m/z69_gradSD |
|---|---|---|---|---|---|---|---|---|---|---|---|---|
| 45 | 2.038 | 0.192 | 2.41 | 1.358 | 8.935 | 4.425 | 0.0151 | 0.0059 | 0.0164 | 0.0034 | 0.1247 | 0.0234 |
| 51 | 2.31 | 0.602 | 1.972 | 0.606 | 7.225 | 2.22 | 0.0165 | 0.002 | 0.0234 | 0.0106 | 0.0519 | 0.0191 |
| 60 | 2.144 | 0.25 | 1.219 | 0.144 | 5.489 | 1.424 | 0.0193 | 0.0004 | 0.0152 | 0.0019 | 0.0557 | 0.0179 |
| 65 | 2.119 | 0.562 | 1.09 | 0.263 | 11.047 | 8.426 | 0.0186 | 0.0077 | 0.0174 | 0.0046 | 0.0556 | 0.0232 |
| 73 | 2.972 | 0.629 | 1.614 | 0.282 | 5.018 | 1.345 | 0.0265 | 0.0017 | 0.0137 | 0.0014 | 0.0536 | 0.0147 |
| 86 | 3.132 | 0.426 | 1.307 | 0.249 | 5.143 | 0.333 | 0.0153 | 0.0012 | 0.0142 | 0.0035 | 0.0523 | 0.0121 |
| 93 | 2.718 | 0.625 | 2.659 | 0.242 | 11.25 | 1.787 | 0.016 | 0.0026 | 0.0324 | 0.0113 | 0.088 | 0.0152 |
| 100 | 3.955 | 0.75 | 4.177 | 1.623 | 15.299 | 7.401 | 0.0211 | 0.0054 | 0.045 | 0.0038 | 0.1835 | 0.0911 |
| 108 | 3.117 | 0.303 | 6.886 | 1.947 | 17.8 | 2.639 | 0.0185 | 0.0056 | 0.056 | 0.0158 | 0.1896 | 0.0584 |
| 114 | 4.696 | 0.115 | 6.722 | 0.427 | 8.787 | 0.274 | 0.0248 | 0.0017 | 0.0539 | 0.0028 | 0.0834 | 0.0211 |
| 122 | 5.807 | 1.051 | 15.477 | 1.311 | 30.994 | 5.812 | 0.0262 | 0.0069 | 0.1188 | 0.0016 | 0.2864 | 0.0014 |
| 246 | 1.637 | 0.207 | 5.763 | 1.323 | 73.75 | 7.653 | 0.0048 | 0.0019 | 0.0309 | 0.0015 | 0.1521 | 0.0179 |
| 253 | 2.757 | 0.424 | 1.593 | 0.418 | 85.071 | 10.635 | 0.0063 | 0.002 | 0.0077 | 0.0028 | 0.146 | 0.0132 |
| 267 | 1.809 | 0.18 | 3.108 | 0.94 | 48.9 | 10.317 | 0.0038 | 0.0006 | 0.0143 | 0.0045 | 0.0809 | 0.0061 |
| 281 | 2.455 | 0.013 | 2.419 | 0.789 | 54.948 | 5.402 | 0.0091 | 0.0018 | 0.0131 | 0.0038 | 0.1654 | 0.0104 |
| 290 | 3.164 | 0.483 | 2.417 | 0.088 | 48.202 | 8.949 | 0.0117 | 0.0012 | 0.0289 | 0.0095 | 0.2704 | 0.0615 |
| 295 | 3.538 | 0.219 | 1.945 | 0.215 | 40.841 | 2.168 | 0.0123 | 0.0018 | 0.0157 | 0.0062 | 0.2367 | 0.0157 |
| 309 | 2.405 | 0.569 | 1.758 | 0.433 | 44.003 | 13.291 | 0.0093 | 0.0012 | 0.0109 | 0.002 | 0.1845 | 0.0295 |
| 167 | 2.285 | 0.456 | 3.732 | 0.217 | 9.401 | 3.993 | 0.0106 | 0.0011 | 0.0247 | 0.0038 | 0.0385 | 0.0128 |
| 175 | 2.047 | 0.296 | 3.449 | 0.909 | 11.478 | 3.48 | 0.0059 | 0.0015 | 0.0199 | 0.0066 | 0.0454 | 0.0156 |
| 189 | 1.489 | 0.008 | 2.926 | 0.166 | 13.419 | 1.607 | 0.0062 | 0.0013 | 0.0191 | 0.0033 | 0.0611 | 0.0028 |
| 196 | 1.53 | 0.194 | 4.154 | 0.404 | 12.535 | 1.457 | 0.0033 | 0.0008 | 0.0196 | 0.003 | 0.041 | 0.0077 |
| 202 | 1.611 | 0.395 | 2.763 | 0.225 | 9.623 | 5.918 | 0.0056 | 0 | 0.0139 | 0.0029 | 0.0302 | 0.0102 |
| 210 | 1.884 | 0.107 | 4.028 | 1.044 | 22.135 | 10.39 | 0.0065 | 0.001 | 0.0253 | 0.0081 | 0.0889 | 0.0511 |
| 216 | 1.311 | 0.321 | 2.672 | 0.669 | 10.201 | 2.859 | 0.0038 | 0.0012 | 0.0121 | 0.0021 | 0.0311 | 0.0041 |
| 223 | 2.574 | 0.107 | 3.64 | 0.955 | 19.882 | 15.169 | 0.0122 | 0.0027 | 0.0219 | 0.0033 | 0.0823 | 0.0318 |

| | | | | | | | | | | | | |
|---|---|---|---|---|---|---|---|---|---|---|---|---|
| 230 | 2.022 | 0.15 | 2.415 | 0.151 | 6.828 | 1.325 | 0.0113 | 0.0028 | 0.0131 | 0.0046 | 0.0304 | 0.011 |
| 245 | 2.61 | 0.382 | 1.178 | 0.189 | 4.274 | 0.835 | 0.0138 | 0.0021 | 0.0043 | 0.0008 | 0.0099 | 0.0037 |
| 251 | 1.554 | 0.163 | 2.01 | 0.188 | 5.115 | 1.161 | 0.0084 | 0.0018 | 0.0077 | 0.0013 | 0.0133 | 0.0043 |
| 258 | 1.817 | 0.325 | 1.546 | 0.135 | 6.275 | 0.914 | 0.013 | 0.0002 | 0.0073 | 0.0008 | 0.0203 | 0.0045 |
| 265 | 2.295 | 0.273 | 1.839 | 0.39 | 8.647 | 0.319 | 0.0177 | 0.0029 | 0.0107 | 0.002 | 0.0366 | 0.0049 |
| 286 | 1.385 | 0.203 | 1.718 | 0.278 | 7.292 | 2.646 | 0.0081 | 0.0013 | 0.0099 | 0.0035 | 0.0281 | 0.0109 |

**Table S8. Data presented in Figure 2c (xxx_prod = VOC production ratio, xxx_SD = standard deviation)**

| DoY | Aceta_prod | Aceta_SD | Aceto_prod | Aceto_SD | Isop_prod | Isop_SD |
|---|---|---|---|---|---|---|
| 46 | 0.0002 | 0.0001 | 0.0002 | 0.0000 | 0.0016 | 0.0003 |
| 52 | 0.0002 | 0.0000 | 0.0003 | 0.0001 | 0.0006 | 0.0002 |
| 61 | 0.0003 | 0.0000 | 0.0002 | 0.0000 | 0.0008 | 0.0003 |
| 66 | 0.0003 | 0.0001 | 0.0002 | 0.0001 | 0.0008 | 0.0003 |
| 73 | 0.0004 | 0.0000 | 0.0002 | 0.0000 | 0.0008 | 0.0002 |
| 90 | 0.0002 | 0.0000 | 0.0002 | 0.0000 | 0.0007 | 0.0002 |
| 94 | 0.0002 | 0.0000 | 0.0004 | 0.0001 | 0.0011 | 0.0002 |
| 101 | 0.0002 | 0.0001 | 0.0005 | 0.0000 | 0.0021 | 0.0010 |
| 108 | 0.0003 | 0.0001 | 0.0008 | 0.0002 | 0.0026 | 0.0008 |
| 114 | 0.0003 | 0.0000 | 0.0006 | 0.0000 | 0.0010 | 0.0002 |
| 122 | 0.0003 | 0.0001 | 0.0016 | 0.0000 | 0.0038 | 0.0000 |
| 247 | 0.0005 | 0.0002 | 0.0031 | 0.0002 | 0.0152 | 0.0018 |
| 254 | 0.0005 | 0.0002 | 0.0006 | 0.0002 | 0.0118 | 0.0011 |
| 268 | 0.0003 | 0.0000 | 0.0010 | 0.0003 | 0.0056 | 0.0004 |
| 282 | 0.0002 | 0.0000 | 0.0003 | 0.0001 | 0.0041 | 0.0003 |
| 290 | 0.0005 | 0.0000 | 0.0011 | 0.0004 | 0.0105 | 0.0024 |
| 297 | 0.0004 | 0.0001 | 0.0006 | 0.0002 | 0.0085 | 0.0006 |
| 309 | 0.0006 | 0.0001 | 0.0007 | 0.0001 | 0.0111 | 0.0018 |
| 167 | 0.0005 | 0.0001 | 0.0011 | 0.0002 | 0.0018 | 0.0006 |
| 175 | 0.0003 | 0.0001 | 0.0008 | 0.0003 | 0.0019 | 0.0007 |
| 189 | 0.0002 | 0.0000 | 0.0005 | 0.0001 | 0.0017 | 0.0001 |
| 196 | 0.0004 | 0.0002 | 0.0016 | 0.0003 | 0.0034 | 0.0006 |
| 202 | 0.0003 | 0.0001 | 0.0010 | 0.0002 | 0.0021 | 0.0007 |
| 210 | 0.0006 | 0.0001 | 0.0022 | 0.0007 | 0.0077 | 0.0044 |
| 216 | 0.0003 | 0.0001 | 0.0008 | 0.0001 | 0.0022 | 0.0003 |
| 223 | 0.0009 | 0.0003 | 0.0019 | 0.0003 | 0.0071 | 0.0027 |
| 230 | 0.0009 | 0.0003 | 0.0012 | 0.0004 | 0.0027 | 0.0010 |
| 245 | 0.0013 | 0.0002 | 0.0004 | 0.0001 | 0.0010 | 0.0004 |
| 251 | 0.0008 | 0.0002 | 0.0007 | 0.0001 | 0.0013 | 0.0004 |
| 259 | 0.0007 | 0.0003 | 0.0005 | 0.0001 | 0.0014 | 0.0003 |
| 265 | 0.0011 | 0.0002 | 0.0006 | 0.0001 | 0.0022 | 0.0003 |
| 286 | 0.0004 | 0.0002 | 0.0004 | 0.0002 | 0.0012 | 0.0005 |

**Table S9. Seasonal production ratio data presented in Figure 4**

| m/z 45 | m/z 45SD | m/z 59 | m/z 59SD | m/z 69 | m/z 69SD | Seasons |
|---|---|---|---|---|---|---|
| 0.000255 | 0.000078 | 0.000225 | 0.000036 | 0.000883 | 0.000352 | Spring pre-bloom |
| 0.000267 | 0.000054 | 0.000779 | 0.000457 | 0.002117 | 0.001149 | Spring bloom |
| 0.000343 | 0.000142 | 0.001243 | 0.000549 | 0.00225 | 0.0006 | Early summer |
| 0.001019 | 0.000183 | 0.000541 | 0.000134 | 0.0014 | 0.00046 | Late summer |
| 0.000418 | 0.000125 | 0.000712 | 0.000295 | 0.009531 | 0.003804 | Autumn |

**Table S10. VOC peak height and production ratio of VOCs presented in Figure 5**

| m/z 45_peak | m/z 45_prod | m/z 59_peak | m/z 59_prod | m/z 69_peak | m/z 69_prod | Vol_culture (mL) |
|---|---|---|---|---|---|---|
| 0 | 0 | 0 | 0 | 0 | 0 | 0 |
| 1.074 | 0.0000442 | 1.967 | 0.0000841 | -0.406 | 0.0000445 | 5 |
| 2.044 | 0.00009 | 4.244 | 0.0001316 | 1.059 | 0.0000977 | 10 |
| 3.618 | 0.0001797 | 7.438 | 0.0002791 | 2.929 | 0.0001714 | 20 |